Molecular Dynamics in the Smectic A and C* Phases in a Long-Chain Ferroelectric Liquid Crystal: 2 H NMR, Dielectric Properties, and a Theoretical Treatment

DATASET · MARCH 2013

CITATIONS
2

READS
17

4 AUTHORS:

Valentina Domenici
Università di Pisa
103 PUBLICATIONS **960** CITATIONS
SEE PROFILE

Marco Geppi
Università di Pisa
121 PUBLICATIONS **1,295** CITATIONS
SEE PROFILE

Carlo Alberto Veracini
Università di Pisa
233 PUBLICATIONS **2,421** CITATIONS
SEE PROFILE

Alex V Zakharov
Russian Academy of Sciences
131 PUBLICATIONS **575** CITATIONS
SEE PROFILE

Molecular Dynamics in the Smectic A and C* Phases in a Long-Chain Ferroelectric Liquid Crystal: ^{2}H NMR, Dielectric Properties, and a Theoretical Treatment

Valentina Domenici,*,† Marco Geppi,† Carlo Alberto Veracini,*,† and Alexandre V. Zakharov‡

Dipartimento di Chimica e Chimica Industriale, Università degli studi di Pisa, via Risorgimento 35, 56126, Italy, and Laboratorium voor Akoestiek en Thermische Fysica, Departement Natuurkunde en Sterrenkunde, Katholieke Universiteit Leuven, Celestijnenlaan 200D, B-3001 Leuven, Belgium

Received: June 7, 2005; In Final Form: July 7, 2005

In this work, the rotational-diffusion coefficients $D_{\|}$ and $D_{\perp}$ for the ferroelectric smectogen (+)-(*S*)-4-[4′-(1-methylheptyloxy)] biphenyl 4-(10-undecenyloxy)benzoate have been studied by means of ^{2}H NMR spectroscopy in the smectic C* phase, using a new theoretical approach (Domenici,V.; Geppi, M.; Veracini, C. A. *Chem. Phys. Lett.* **2003**, *382*, 518). The analysis of spin−lattice relaxation times has been performed in terms of the diffusional constant and the activation energy of the internal and overall molecular-reorientational motions, and the results are compared to the smectic A (SmA) phase. Moreover, from the ^{2}H NMR data in the SmA phase, the dielectric permittivity and the dielectric relaxation time functions τ_{mn}^{L} are investigated using a theoretical approach. The longitudinal and transverse components of the real $\mathscr{R}\chi_{\gamma}(\omega)$ and imaginary $\chi_{\gamma}(\omega)$ ($\gamma = \|, \perp$) parts of the complex susceptibility tensor and the nematic-like rotational-viscosity coefficients, λ_2 and λ_5, are calculated.

Introduction

NMR and dielectric spectroscopy (DS) are two of the most important techniques for investigating molecular dynamics in liquid crystals. Nuclear relaxation and dielectric relaxation both can give dynamic information over a wide frequency range by changing their characteristic measurement frequencies; in the case of NMR, for instance, spin−spin and spin−lattice relaxation times are used for characterizing slower (0.1 Hz to 10^2 kHz) and faster (10 MHz to 10^3 GHz) motions, respectively,[1] while different instrumental apparatus allow the frequency range of 1 kHz $\leq \omega/2\pi \leq$ 1 GHz in DS to be covered.[2] Despite this, the comparison between the results obtained from the two spectroscopies is quite difficult as a result of their intrinsically different nature. In particular, NMR probes the system at a microscopic level, measuring properties of nuclei present in different positions within the molecule, while DS monitors a macroscopic property of the system. Therefore, NMR and DS experimental data are usually determined by different sets of molecular motions. Moreover, NMR and DS usually deal with "rank-two" and "rank-one" tensorial properties, respectively. The perspective of quantitatively comparing quantities determined by the two techniques is, however, very attractive to reciprocally validate the reliability of this dynamic information. Some efforts have been recently done, especially in the comparison between ^{2}H spin−lattice relaxation and dielectric relaxation in the nematic phase[3−6] and smectic A (SmA) phase[4] of thermotropic liquid crystals.

^{2}H Zeeman (T_{1Z}) and quadrupolar (T_{1Q}) spin−lattice relaxation times can be quite easily measured when suitable selectively labeled molecules are available; moreover, they can be interpreted in terms of intramolecular interactions only. Models have been developed that allow the experimental relaxation times to be quantitatively analyzed to get individual diffusional coefficients for overall molecular motions (i.e., spinning and tumbling), internal reorientations of molecular fragments, and collective orientational-order fluctuations.

On the other hand, dielectric-relaxation experimental data usually consist of the frequency-dependent dielectric permittivity, measured using different techniques depending on the frequency range and/or the degree of orientation of the samples.[2] The relaxation times for the two main relaxation processes (high frequency and low frequency) are then derived resorting to a Debye-type relaxation theory.

Relationships have been proposed for uniaxial phases on the basis of several models that link the dielectric relaxation times to the diffusional coefficients for the overall molecular motions (tumbling and spinning). The encouraging results recently obtained in comparing DS and NMR relaxation measurements justify further investigations in both the theoretical analysis of the experimental data and the extension of such studies to other mesogens, such as ferroelectric liquid crystals.

In regard to the biaxial phases such as the ferroelectric smectic C* (SmC*) phase, several difficulties in linking them to the dynamic parameters exist even though relaxation times can also be measured.[7] These difficulties are both theoretical and experimental and are either due to the phase biaxiality or due to the dependence of the relaxation times on the polar angles defining the position of the local phase director with respect to the external magnetic field.[8] In fact, on one side, theoretical models taking into account phase biaxiality are quite complex,[9,10] while on the other side, such a model would require an unavailable large set of experimental data. In this paper, the dynamic study is extended to the biaxial SmC* phase of the ferroelectric smectogen (+)-(*S*)-4-[4′-(1-methylheptyloxy)] biphenyl 4-(10-undecenyloxy)benzoate (11EB1M7) by using a new approach to analyze ^{2}H spin−lattice relaxation times in

* Corresponding authors. Valentina Domenici: phone number, +39-0502219289; fax number, +39-0502219260; e-mail, valentin@dcci.unipi.it. Carlo Alberto Veracini: phone number, +39-0502219235; fax number, +39-0502219260; e-mail, verax@dcci.unipi.it.

† Università degli studi di Pisa.

‡ Katholieke Universiteit Leuven.

10.1021/jp053028b CCC: $30.25
Published on Web 09/10/2005

tilted smectic phases in terms of dynamic parameters for individual molecular and internal motions.[11,12] This new approach allows the quantitative analysis of relaxation times in tilted smectic phases by means of the existing theoretical models on the basis of the assumption of phase uniaxiality, but taking into account the effects of the tilt angle on the measured relaxation times. The obtained results are discussed in terms of the activation energies and the diffusional coefficients of the overall molecular and internal motions, and they are compared with data previously found in the SmA phase.[13] It's important to notice that the analysis here reported is self-consistent, and its validity is related to the availability of measurements performed on two labeled isotopomers at three Larmor frequencies, thus, allowing a global fitting without fixing any sensitive parameters.

Moreover, dielectric properties such as correlation times and transverse and longitudinal components of the real and imaginary part of the complex susceptibility tensor are calculated by using a theoretical approach starting from the ^{2}H NMR results for the ferroelectric smectogen in its SmA phase. Measurements for smectic viscosities are presently rather scarce, and the theoretical information about these constants is very useful. Equations governing the flow behavior of SmC* liquid crystals demand 20 viscosity coefficients. In this work, the nematic-like viscosity coefficients are calculated for the first time from ^{2}H NMR results for 11EB1M7 in the SmC* phase.

^{2}H NMR Study of Molecular Dynamics: Theory

The relationships that link the spin−lattice relaxation times T_{1Z} and T_{1Q} to the spectral densities $J_1(\omega_0)$ and $J_2(2\omega_0)$ are[14]

$$\frac{1}{T_{1Z}(\Omega)} = J_1(\omega_0,\Omega) + 4J_2(2\omega_0,\Omega) \tag{1}$$

and

$$\frac{1}{T_{1Q}(\Omega)} = 3J_1(\omega_0,\Omega) \tag{2}$$

where ω_0 is the Larmor frequency and $\Omega = \theta, \phi$ indicates the polar angles of the phase director in the laboratory frame defined by the external magnetic field.

Several models have been proposed to interpret the spectral densities in uniaxial phases at $\theta = 0$ (i.e., with the phase directors aligned to the external magnetic field) in terms of dynamic parameters of individual internal and overall molecular motions. When the model developed by Tarroni and Zannoni[10,15] is used in the uniaxial approximation for the overall molecular reorientations and the strong collision model[16] is used for the internal motions, which are considered superimposed, the following equation can be derived for the spectral densities of the *i*th deuteron:

$$J^i_{mL}(n\omega_0) = \frac{3\pi^2}{2}(\nu_q)^2 \sum_{m_M=-2}^{2} \sum_{m_R=-2}^{2} c_{m_L,m_M}[d^2_{m_R,0}(\beta_{i,Q_i})]^2[d^2_{m_M,m_R} \times (\beta_{M,i})]^2 \sum_j a^{(j)}_{m_L,m_M} \frac{(\tau^{(j)}_{m_L,m_M})^{-1} + (1-\delta_{mR})D_i}{(n\omega_0)^2 + [(\tau^{(j)}_{m_L,m_M})^{-1} + (1-\delta_{mR})D_i]^2} \tag{3}$$

where the autocorrelation functions for the overall molecular motions have been expressed as a sum over j of decreasing exponential functions with time constants $\tau^{(j)}_{m_L,m_M}$ through the coefficients $a^{(j)}_{m_L,m_M}$, $b^{(j)}_{m_L,m_M}$, and c_{m_L,m_M} that have been calculated as a function of the principal order parameter (OP) S_{zz} for a Maier−Saupe potential in ref 17. ν_q is the quadrupolar coupling constant, $d^2_{r,s}$ are the reduced Wigner matrices, β_{i,Q_i} is the angle between the C−D bond and the axis about which the internal rotation takes place, $\beta_{M,i}$ is the angle between this axis and the molecular long axis, and D_i is the diffusion coefficient relative to the internal motion of the corresponding fragment. The correlation times $\tau^{(j)}_{m_L,m_M}$ are expressed in terms of the diffusion coefficients $D_\parallel$ and $D_\perp$, the principal components of the diffusion tensor diagonalized in a molecular frame, describing the molecular spinning and tumbling motions, respectively:

$$\frac{1}{\tau^{(j)}_{m_L,m_M}} = \frac{6D_\perp}{b^{(j)}_{m_L,m_M}} + m^2_M(D_\parallel - D_\perp) \tag{4}$$

Order director fluctuations (DF) can also affect the spin−lattice relaxation, but they can be considered uncoupled to reorientational motions; their contribution to spectral densities, predicted by the theory developed by Pincus,[18] is null for $J_2(2\omega_0)$ and given by the following equation for $J_1(\omega_0)$:

$$J^{DF}_1(\omega_0) = \frac{3\pi^2}{2}(\nu_q)^2[d^2_{00}(\beta_{i,Q_i})]^2[d^2_{00}(\beta_{M,i})]^2(S_{ZZ})^2 T\frac{a_{DF}}{\sqrt{\omega_0}} \tag{5}$$

where S_{ZZ} is the molecular OP and the factor a_{DF} depends on macroscopic parameters such as the viscosity coefficient, the average Frank elastic constant, and the autodiffusion translational constant. It must be pointed out that the contribution of DF to ^{2}H spin−lattice relaxation in rodlike liquid crystals may be very small, either because of geometrical reasons (for instance, when deuterated aromatic moieties are considered, the term $d^2_{00}(\beta_{i,Q_i})$ is very small because β_{i,Q_i} is very close to the magic angle) or because the characteristic frequencies of DF are much smaller than the Larmor frequency. The contribution to the relaxation of other very slow collective motions peculiar to chiral smectic phases, such as soft and Goldstone modes, can be safely neglected on the basis of frequency-scale arguments.

When a tilted smectic phase is considered, θ is different from zero and the relaxation times are, in principle, dependent on both the polar angle θ and the polar angle ϕ.

On the other hand, an analysis of experimental relaxation times on this basis is impossible for both experimental and theoretical reasons.

For instance, in a chiral SmC* phase, the phase director describes a helicoidal structure along the normal to the smectic planes (z axis); that is, the tilt angle θ always remains fixed, while the azimuthal angle ϕ assumes different values depending on the z coordinate. However, equivalent deuterons of different molecules corresponding to different smectic planes and, therefore, different ϕ values give exactly the same quadrupolar doublet in the ^{2}H NMR spectrum, thus, creating indistinguishable results. Consequently, only one average relaxation decay can be recorded for all the equivalent deuterons of the phase.

On the other hand, even if different experimental values for the relaxation times could be obtained for different ϕ values, no suitable theories would be actually available to analyze them in terms of dynamic parameters. An assumption that allows us to treat the experimental relaxation times in tilted smectic phases consists of considering them independent from the azimuthal angle ϕ. This assumption, which could seem too drastic, is indeed supported by the experimental evidence of a mono-exponential decay for all the ^{2}H spin−lattice measurements performed so far on tilted smectic phases, indicating that, if

the ϕ dependence existed, it would be, nevertheless, too small to be revealable.[11,12]

By neglecting the ϕ dependence, the following equations can be derived:[9]

$$J_1(\omega,\theta) = \left(\frac{3\cos^2\theta\sin^2\theta}{2}\right)J_0(\omega,0) + \left(\frac{1-3\cos^2\theta+4\cos^4\theta}{2}\right)J_1(\omega,0) + \left(\frac{1-\cos^4\theta}{2}\right)J_2(\omega,0) + -\sqrt{6}(\cos^2\theta\sin^2\theta)J_{2,0}(\omega,0) - \left(\frac{1-5\cos^2\theta+4\cos^4\theta}{2}\right)J_{1,-1}(\omega,0) - \left(\frac{1-\cos^2\theta}{2}\right)^2 J_{2,-2}(\omega,0) \quad (6)$$

$$J_2(\omega,\theta) = \left(\frac{3(1-\cos^2\theta)^2}{8}\right)J_0(\omega,0) + \left(\frac{1-\cos^4\theta}{2}\right)J_1(\omega,0) + \left(\frac{1+6\cos^2\theta+\cos^4\theta}{8}\right)J_2(\omega,0) + \sqrt{6}\left(\frac{1-\cos^4\theta}{4}\right)J_{2,0}(\omega,0) + \left(\frac{1-2\cos^2\theta}{2}\right)J_{1,-1}(\omega,0) + \left(\frac{1-\cos^2\theta}{8}\right)J_{2,-2}(\omega,0) \quad (7)$$

where the uniaxial spectral densities J_0, J_1, and J_2 and the biaxial spectral densities $J_{2,0}$, $J_{1,-1}$, and $J_{2,-2}$ appear. These last spectral densities can be neglected in the uniaxial approximation as previously stated.[11]

Eqs 6 and 7, also used in angular dependence studies,[19] link the experimental spectral densities $J_1(\omega,\theta)$ and $J_2(\omega,\theta)$ to the spectral densities at $\theta = 0$, which are to be used within the theoretical models. The spectral densities measured by the Jeener−Broekaert experiment for each type of deuteron at a given temperature are only two [$J_1(\omega_0,\theta)$ and $J_2(2\omega_0,\theta)$], and, therefore, the six spectral densities at $\theta = 0$ [$J_1(0,0)$, $J_2(0,0)$, $J_1(\omega_0,0)$, $J_2(\omega_0,0)$, $J_1(2\omega_0,0)$, and $J_2(2\omega_0,0)$] cannot be directly determined from eqs 6 and 7. However, if eq 3 is inserted within eqs 6 and 7, without the biaxial spectral densities, and a global target approach is used, which assumes an Arrhenius behavior for the various diffusion coefficients [$D_k(T) = D_k^\infty e^{-E_a^k/kT}$, the label k indicating the type of motion], the best values of the parameters D_k^∞ and E_a^k can be determined by applying a suitable nonlinear least-squares fitting procedure.[20]

^{2}H NMR Analysis of the Ferroelectric Phase: Experimental Results

Sample. The sample under investigation is the 11EB1M7. Two isotopomers were available, labeled on either the phenyl or the biphenyl moiety of the mesogenic core (11EB1M7-d_2 and 11EB1M7-d_8) as shown in Figure 1a,b. The synthesis and characterization of the mesomorphic behavior of all of them are reported in refs 21−23, respectively. The following phase behaviors were respectively found for the mesogens 11EB1M7-d_2 and 11EB1M7-d_8 by optical microscopy and differential scanning calorimetry:

I 115.9 °C BPI 113.2 °C N* 108.0 °C TGBA* 102.0 °C SmA 91.0 °C SmC* 76.9 °C smectic I* (SmI*) 72.2 °C Cr

I 111.4 °C BPI 109.8 °C N* 107.4 °C TGBA* 103.1 °C SmA 90.3 °C SmC* 68.7 °C SmI* 63.5 °C Cr

As reported in ref 23, in the NMR study, slightly lower-phase transition temperatures were found and the SmI* phase could not be identified.

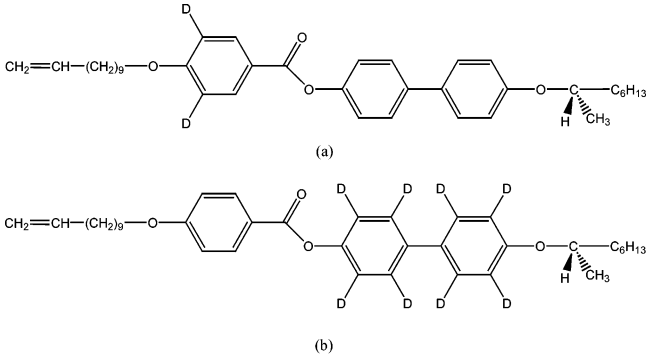

Figure 1. Molecular structure of the ferroelectric smectogens 11EB1M7-d_2 (a) and 11EB1M7-d_8 (b).

^{2}H NMR. ^{2}H Zeeman (T_{1Z}) and quadrupolar (T_{1Q}) spin−lattice relaxation times were recorded by means of a broadband version[24] of the Jeener−Broekaert pulse sequence.[25] The relaxation measurements were recorded on a Varian VXR-300 spectrometer working at 46 MHz, on a Varian XL100 spectrometer interfaced with a Stelar DS−NMR acquisition system working at 15 MHz, and on a home-built spectrometer working at 58 MHz.

The structure, orientational order, and relaxation study in the SmA phase of the smectogen 11EB1M7 by deuterium NMR are presented in ref 23, and details of the relaxation measurements have been reported in refs 23 and 13.

Data Analysis. All relaxation data are analyzed by using a modified version of the CAGE package, including the treatment of the biaxial phases according to the approach developed in our group.[20]

Results and Discussion. ^{2}H spin−lattice relaxation times at three Larmor frequencies and for two different deuteron types were available that were previously analyzed in terms of diffusional coefficients in the uniaxial SmA phase using Tarroni and Zannoni, strong collision, and Pincus models for overall, internal, and collective motions, respectively. This analysis has been extended here to the whole SmC* range.

In this case, the availability of a large set of experimental data allowed us to overcome the need to resort to the Perrin model[26] for fixing $D_\parallel/D_\perp$: in both the SmA and the SmC* phases, the global fitting could be carried out without fixing any parameters, resulting in well-determined diffusional coefficients, even for the tumbling motion.

In the SmC* phase, the fitting was performed using 112 experimental points (11 temperatures at 58 and 46 MHz and 6 temperatures at 15 MHz for two isotopomers) to get 9 best-fitting parameters (pre-exponential factor and activation energy for molecular spinning and tumbling and for phenyl and biphenyl ring rotation, as well as the a_{DF} coefficient). In agreement with a previous orientational-order study and on the basis of the analysis of ^{2}H quadrupolar and ^{2}H−^{1}H dipolar splittings,[23] the angle β_{i,Q_i} was taken as 60° for all the deuterons and the molecular long axis was assumed to be parallel to the para axis of the biphenyl fragment. Within the SmC* phase, the OP S_{ZZ} ranges from 0.738 to 0.756 and the tilt angle, evaluated from the ^{2}H NMR spectra for the long molecular axis, increases from 12.6 to 18.5° by decreasing the temperature. Figure 2 shows the trend of the orientational-order paramenter S_{ZZ} ($\equiv S_2$) as obtained from ^{2}H NMR analysis. The angle between the molecular long axis and the para axis of the phenyl fragment was calculated from the ratio of the OPs of the two aromatic fragments, taking into account the tilt angle, and ranges from 5.0 to 8.2 ± 0.5° within the SmC* phase.

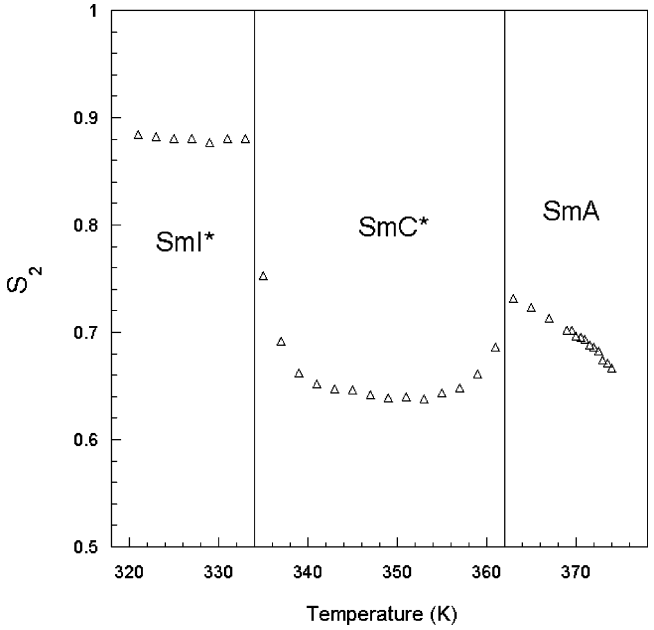

Figure 2. Orientational OP S_2 of the ferroelectric smectogen 11EB1M7 by means of ^{2}H NMR.

The comparison between experimental and calculated spectral densities in both the SmA and the SmC* phases (see Figure 3a,b for 11EB1M7-d_2 and 11EB1M7-d_8 data, respectively) reveals a substantially good agreement. The biggest deviations are obtained for the data recorded at 15 MHz, which are indeed affected by the largest experimental errors because of the lower sensitivity.

The diffusion coefficients obtained for the spinning and tumbling molecular motions as well as for the internal motions of the phenyl and the biphenyl fragments are reported in Figure 4.

A value of about 1.0×10^{-8} K^{-1} $s^{1/2}$ $rad^{-3/2}$ was found for a_{DF}. This is of the same order of magnitude as that previously found in the SmA phase and corresponds to very small contributions of order DF to the spectral densities of the aromatic deuterons (less than 5.5 and 8% for phenyl and biphenyl deuterons, respectively).

While the diffusion coefficients, relative to the rotations of phenyl and biphenyl moieties and to the spinning motion, do not show any discontinuities passing from the SmA to the SmC* phase, this is not the case for the tumbling motion, the diffusion coefficient of which abruptly decreases by about 1 order of magnitude at the phase transition. Moreover, the activation energies of the two internal and molecular tumbling motions remarkably increase on entering the SmC* phase (from 35 to 78 kJ/mol, from 20 to 61 kJ/mol, and from 40 to 119 kJ/mol for phenyl rotation, biphenyl rotation, and molecular tumbling, respectively), while that of the spinning motion remains substantially unchanged. As a result, the molecular spinning, with a diffusion coefficient of about 1.0×10^9 s^{-1}, becomes the faster motion at the low-temperature limit of the SmC* phase, being of the same order of magnitude of the biphenyl rotation and about 1 order and 3 orders of magnitude faster than phenyl rotation and tumbling, respectively.

Also, in this case, the fitting did not give a satisfactory reproduction of the experimental data when using the small-step rotational-diffusion model instead of the strong collision model for describing either the biphenyl or phenyl internal motions.

The results obtained, thanks to the availability of several experimental frequencies, are not ill-conditioned by a priori

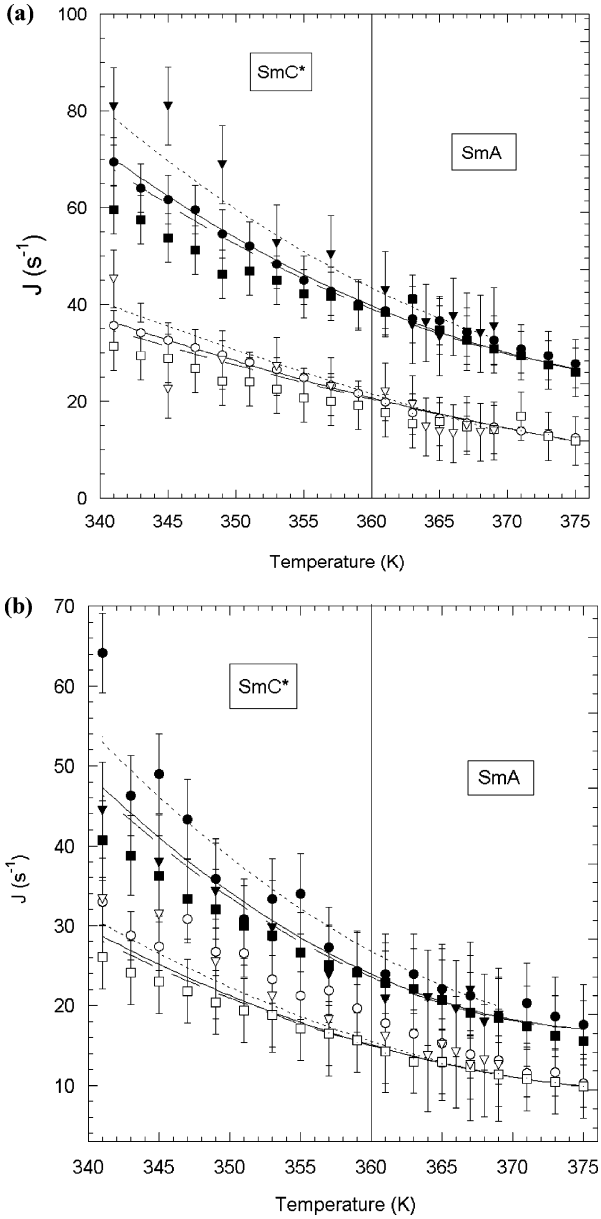

Figure 3. Experimental (symbols) and calculated (lines) spectral densities (s^{-1}) in the SmA and SmC* phases vs temperature (K). Full and empty symbols indicate $J_1(\omega_0,\theta)$ and $J_2(2\omega_0,\theta)$, respectively. Triangles, squares, and circles refer to data at 15, 58, and 46 MHz, respectively. Dotted, dashed, and solid curves refer to spectral densities calculated at 15, 58, and 46 MHz, respectively. Parts a and b refer to 11EB1M7-d_2 and 11EB1M7-d_8, respectively.

assumptions, such as having fixed the value of the $D_\parallel/D_\perp$ ratio and neglected the contribution of order DF, and the best-fitting parameters so obtained are affected by relatively small errors (less than 10% for $D_{\parallel}$, 5% for $D_{(phen)}$, 8% for $D_{(biph)}$, and 35% for $D_\perp$). As shown in Figure 4, the diffusional coefficient for the tumbling motion is characterized by a sensitive jump to a lower value that cannot be justified in terms of the higher experimental error related to the determination of such a parameter ($\Delta = 35\%$) relative to the other parameters. A hypothesis to explain this trend is that it could be related to the tilt of the molecules relative to the magnetic field direction, but at the moment, neither theories nor models are able to explain this observed result. Moreover, this behavior seems to be peculiar to this smectogen even though only a few ferroelectric molecules have been investigated by means of this technique, and the results reported in the literature refer to single

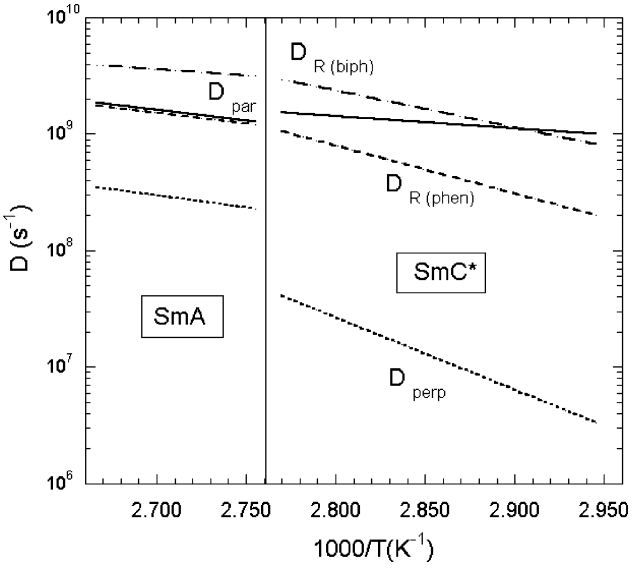

Figure 4. Diffusion coefficients D_{par}, D_{perp}, $D_{(phen)}$, and $D_{(biph)}$ (s^{-1}) reported on a logarithmic scale vs $1000/T$ (K^{-1}) for the smectogen 11EB1M7 in the SmA and SmC* phases.

frequency studies and to more restricted experimental data sets. To confirm and explain this significant dynamic behavior, other smectogens are under study in our lab.

Relaxation Times and Dielectric Properties in the SmA Phase

Rotational dynamics of molecules in anisotropic phases can be described by the small-step diffusion model.[10] This model is based on the assumption that molecular reorientations proceed through a random sequence of infinitesimal angular jumps.

In general, however, the rotational motion of a uniaxial molecule in a liquid-crystal phase is conveniently characterized using orientational time-correlation functions (TCFs):

$$\phi^L_{mn}(t) = \langle D^L_{mn}{*}[\Omega(0)] D^L_{mn}[\Omega(t)]\rangle \tag{8}$$

where $D^L_{mn}(\Omega)$ is the Wigner rotational matrix element of rank L and $\Omega = (\alpha, \beta, \gamma)$ is a set of time-dependent Euler angles that define the orientation of the molecular-axis system relative to the director frame. The index m is related to the director-coordinate system, whereas molecular properties are dictated by the index n.

Different spectroscopic methods correspond to correlation functions with different values of L; the first-rank ($L = 1$) TCFs are relevant for infrared and dielectric spectroscopies while TCFs with $L = 2$ appear, for example, in the expressions for nuclear-spin relaxation rates and Raman band shapes.

The initial values of the TCFs, $\langle D^L_{mn}{*}[\Omega(0)] D^L_{mn}[\Omega(t)]\rangle$, can be expressed in terms of the orientational OPs. Notice that the first-rank TCFs at $t = 0$ depend on the second-rank OP S_2 ($\equiv S_{ZZ}$) only, while for the second-rank correlation function, both S_2 and the fourth-rank S_4 are required.

In general, the correlation functions may be written as infinite sums of decaying exponentials. Here, we employ a single-exponential approximation:[1,15]

$$\phi^L_{mn}(t) = \phi^L_{mn}(\infty) + [\phi^L_{mn}(0) - \phi^L_{mn}(\infty)]\mathrm{e}^{-(t/\tau_{mn}{}^L)} \tag{9}$$

To determine the molecular reorientations, we need a model for the interpretation of the relaxation times, τ^L_{mn}, in terms of rotational constants.[27,28] On the basis of the short time expansion of the TCFs, the following expression for the relaxation times was proposed:

$$\frac{1}{\tau^L_{mn}} = c^L_{mn} D_\perp + n^2(D_\parallel - D_\perp) \tag{10}$$

where the coefficients c^L_{mn}, which depend on the OPs, are tabulated in ref 27 and $D_\parallel$ and $D_\perp$ are the principal components of the diffusion tensor diagonalized in a molecular frame, describing the molecular spinning and tumbling motions, respectively. We note that τ^1_{00} and τ^1_{10} are solely determined by the tumbling motion:

$$\tau^1_{00} = \left[D_\perp \frac{2 - 2S_2}{1 + 2S_2}\right]^{-1} \tag{11}$$

$$\tau^1_{10} = \left[D_\perp \frac{2 + 2S_2}{1 - 2S_2}\right]^{-1} \tag{12}$$

whereas τ^1_{01} is related to $D_\parallel$ and $D_\perp$ by

$$\tau^1_{01} = \left[D_\parallel + D_\perp \frac{1 + 2S_2}{1 - S_2}\right]^{-1} \tag{13}$$

Having obtained a set of the relaxation times τ^1_{mn}, it is now possible to describe the dielectric relaxation processes.

The complex dielectric permittivity tensor $\epsilon_{ij}(\omega) = \mathscr{R}\epsilon_{ij}(\omega) - i\mathscr{I}\epsilon_{ij}(\omega)$ has been measured for a number of liquid crystal compounds in a wide frequency range and shows a Debye-type relaxation at microwave frequencies (1 kHz $\leq \omega/2\pi \leq$ 1 GHz).[29]

For the SmA phase, in the laboratory coordinate system XYZ, where the Z axis coincides with the phase director $\vec{n}$, there are only two independent components of the tensor $\epsilon_{ij}(\omega)$, one perpendicular $\epsilon_\perp(\omega) = \epsilon_{XX}(\omega) = \epsilon_{YY}(\omega)$ and one parallel $\epsilon_\parallel(\omega) = \epsilon_{ZZ}(\omega)$ to the director $\vec{n}$. In this case, when the intermolecular correlations are ignored, one can write the expression for the components of the normalized complex susceptibility tensor $\chi_{ij}(\omega)$ in the form[5,30]

$$\chi_\gamma(\omega) = \frac{\epsilon_\gamma(\omega) - \epsilon_{\gamma\infty}}{\tilde{R}_\gamma(\omega)} = C_\gamma(0) - i\omega\int_0^\infty C_\gamma(t)\mathrm{e}^{(-i\omega t)}\,\mathrm{d}t = C_\gamma(0) - i\omega\tilde{C}_\gamma(i\omega) \tag{14}$$

where $\tilde{R}_\gamma(\omega) = 4\pi\mu^2\rho/k_\mathrm{B}T$, $R_\gamma(\omega)$ and $R_\gamma(\omega)$ are the frequency-dependent factors of the internal field, k_B is the Boltzmann constant, T is the temperature, ρ is the density, and $\epsilon_{\gamma\infty}$ is the high-frequency limit of the components of the tensor, $\epsilon_{ij}(\omega)$ and $\gamma = \parallel, \perp$.

Here, $C_\gamma(t)$ and $\tilde{C}_\gamma(i\omega)$ are the components of the dipole autocorrelation-function tensor and their Fourier transforms, respectively, and may be represented[5,30] as

$$C_\parallel(t) = \langle \mu_{ZZ}(0)\,\mu_{ZZ}(t)\rangle = \phi^1_{00}(t) \tag{15}$$

$$C_\perp(t) = \langle \mu_{xx}(0)\,\mu_{xx}(t)\rangle = \langle \mu_{yy}(0)\,\mu_{yy}(t)\rangle = \phi^1_{10}(t) \tag{16}$$

where ϕ^1_{i0} ($i = 0, 1$) are the first-rank TCFs and $\mu_{\alpha\alpha}$ are the projections of the unit vector μ along the dipole moment on the laboratory axis α ($\alpha = x, y, z$).

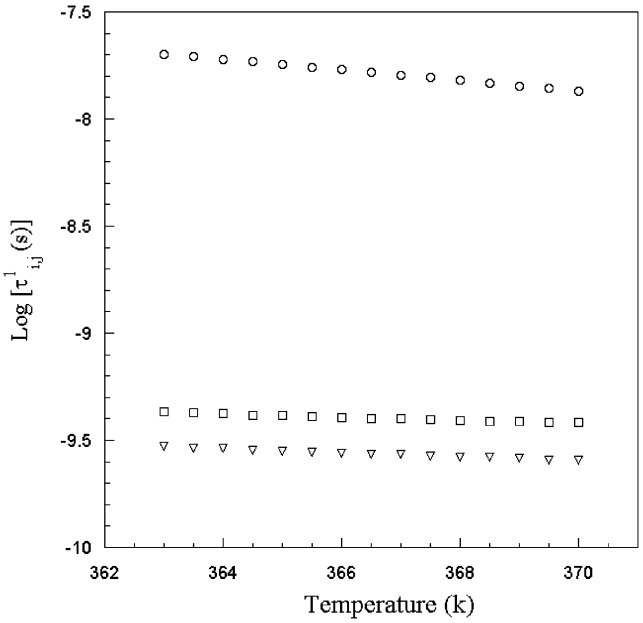

Figure 5. Temperature dependence of the logarithm of relaxation times τ^1_{ij} (s) calculated using equations in the text. Circles, squares, and triangles refer to τ^1_{00}, τ^1_{10}, and τ^1_{01}, respectively.

Using eqs 15 and 16,

$$\phi^1_{00}(t) = \phi^1_{00}(0)\mathrm{e}^{(-t/\tau_{00}{}^1)} = \frac{1 + 2S_2}{3}\mathrm{e}^{(-t/\tau_{00}{}^1)} \qquad (17)$$

and

$$\phi^1_{10}(t) = \phi^1_{10}(0)\mathrm{e}^{(-t/\tau_{10}{}^1)} = \frac{1 - S_2}{3}\mathrm{e}^{(-t/\tau_{10}{}^1)} \qquad (18)$$

we may derive the expressions for the components of the tensor $\chi_\gamma(\omega)$ with $\gamma = ||, \perp$ (eq 13) interpreted in the framework of the Brownian motion of a particle in a mean-field potential $U(\Omega)$ as

$$\chi_{||}(\omega) = \mathscr{R}\chi_{||}(\omega) - i\mathscr{I}\chi_{||}(\omega) = \frac{1 + 2S_2}{3}\left(1 - \frac{i\omega\tau^1_{00}}{1 + i\omega\tau^1_{00}}\right) \qquad (19)$$

and

$$\chi_{\perp}(\omega) = \mathscr{R}\chi_{\perp}(\omega) - i\mathscr{I}\chi_{\perp}(\omega) = \frac{1 - S_2}{3}\left(1 - \frac{i\omega\tau^1_{10}}{1 + i\omega\tau^1_{10}}\right) \qquad (20)$$

The relaxation times τ^1_{mn} (m, $n = 0$, 1) are calculated in the temperature range corresponding to the SmA phase for the smectogen 11EB1M7 on the basis of eqs 10 and 11 and using the values of the OP, S_2, and the rotational-diffusion coefficients (RDCs) $D_{||}$ and $D_\perp$ obtained from the analysis of NMR measurements (Figure 5).

Having obtained the relaxation time functions, it is now possible to calculate, using eqs 19 and 20, the complex dielectric susceptibility coefficients $\chi_\gamma(\omega)$, $\gamma = ||, \perp$.

The results of the calculations of the longitudinal dielectric dispersion $\mathscr{R}\chi_{||}(\omega)$ and adsorption $\mathscr{I}\chi_{||}(\omega)$ for 11EB1M7 chiral molecules performed at several temperatures (T = 370, 369, 368, 367, and 366 K) are shown in Figures 6 and 7.

The transverse dielectric dispersion $\mathscr{R}\chi_\perp(\omega)$ and adsorption $\mathscr{I}\chi_\perp(\omega)$ for the same thermodynamic conditions are shown in Figures 8 and 9.

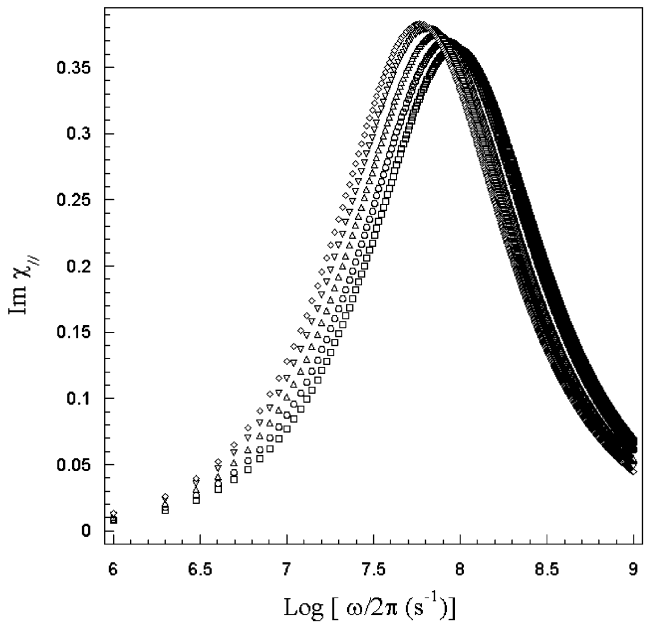

Figure 6. Imaginary part of the longitudinal susceptibility at four temperatures [T = 370 (squares), 369 (circles), 368 (triangles up), 367 (triangles down), and 366 K (diamonds)] as a function of the logarithm of $\omega/2\pi$ (s^{-1}).

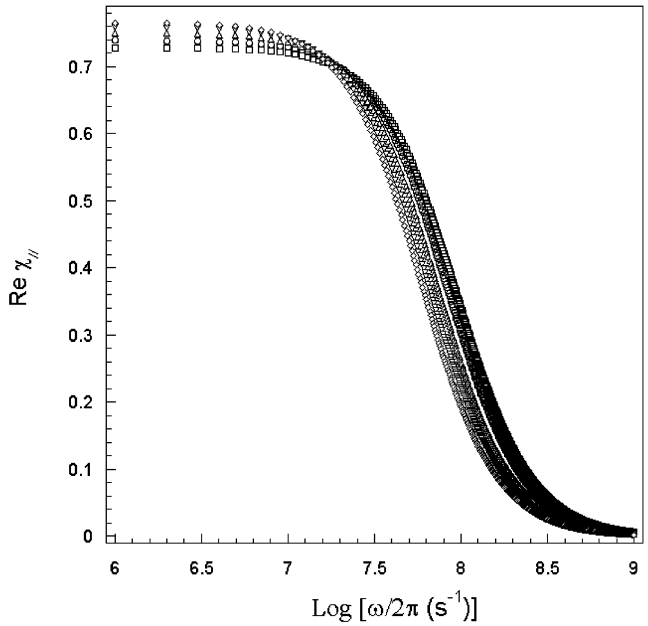

Figure 7. Real part of the longitudinal susceptibility at four temperatures [T = 370 (squares), 369 (circles), 368 (triangles up), 367 (triangles down), and 366 K (diamonds)] as a function of the logarithm of $\omega/2\pi$ (s^{-1}).

The longitudinal and transverse dispersions $\mathscr{R}\chi_\gamma(\omega)$ ($\gamma = ||$, $\perp$) show magnitudes that decrease with the growth of the temperature. The calculation of the longitudinal dispersion shows (see Figure 7) a decrease of up to 5 % of the dispersion intensity in the temperature range from 370 to 366 K, whereas their dielectric loss values (see Figure 6) are characterized by a decrease of the adsorption intensity with increasing temperature in the smectic phase. This shows that the influence of the strong dipole correlations prevails over steric interactions among 11EB1M7 chiral molecules in the smectic phase.

The magnitudes of the longitudinal-dielectric-loss spectra $\chi_{||}(\omega)$ decrease with the growth of the temperature and have one loss peak which shifts in the higher frequency region. The

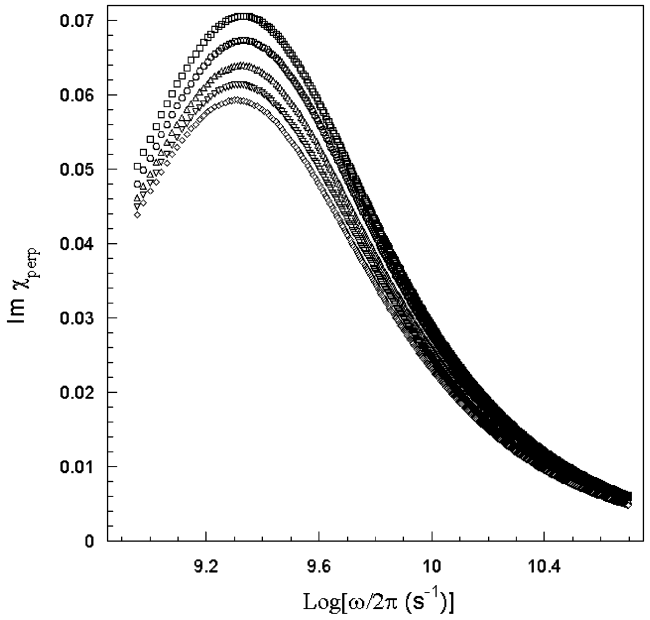

Figure 8. Imaginary part of the transverse susceptibility at four temperatures [$T = 370$ (squares), 369 (circles), 368 (triangles up), 367 (triangles down), and 366 K (diamonds)] as a function of the logarithm of $\omega/2\pi$ (s^{-1}).

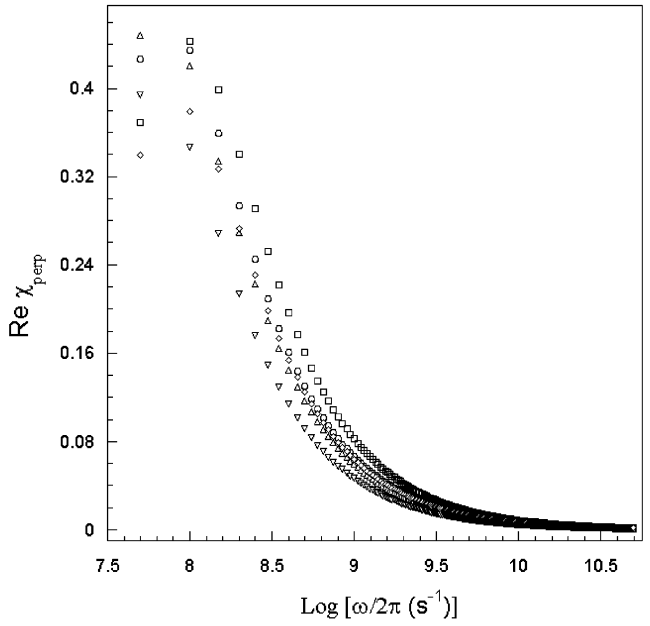

Figure 9. Real part of the transverse susceptibility at four temperaures [$T = 370$ (squares), 369 (circles), 368 (triangles up), 367 (triangles down), and 366 K (diamonds)] as a function of the logarithm of $\omega/2\pi$ (s^{-1}).

magnitudes of the transverse-dielectric-loss spectra $\chi_{\perp}(\omega)$, on the contrary, increase with increasing temperature, and its loss peak remains at the same frequency of ≈1.2 GHz.

Formulas for the Nematic-like Viscosities of the SmC* Phase

During the past few years, a great deal of attention has been focused on the flow dynamics of SmC* liquid crystals in a shear flow.[31−33] It has been shown that the general theory for the description of the macroscopic flow properties of the SmC* system demands 20 viscosity coefficients.

In accordance with the stress tensor expression σ_{ij} (see, for instance, eqs 3.14 and 3.15, ref 32) for the SmC* phase, each of these 20 coefficients can be classified into one of four groups. The first group consists solely of one contribution which is independent both of the director $\hat{n}$ and of their projection $\hat{c}$ onto the smectic plane[33] and, therefore, corresponds to the usual isotropic contribution to the viscous stress tensor σ_{ij} (see eq 6.219, ref 33). The second group consists of those viscosities that are connected to the director $\hat{n}$ and independent of the vector $\hat{c}$. This group consists of four viscosities (see eq 6.220) whose terms, being independent of $\hat{c}$, suggest that the smectic tilt angle $\theta = 0$, and for this reason, they are called SmA-like viscosities. The third group of viscosities is connected to the terms which only depend on the vector $\hat{c}$ and consists of four contributions (see eq 6.221). They have been designated as nematic-like viscosities (μ_3, μ_4, λ_2, and λ_5 in the notation of the eq 6.221, ref 33). The fourth group consists of the remaining 11 viscosities, which are associated with coupling terms because they depend on both $\hat{n}$ and $\hat{c}$. Comparisons between the five Leslie viscosity coefficients of the nematic liquid crystal[34,35] and the corresponding nematic-like viscosity coefficients of a SmC* liquid crystal[31−33] gives us

$$\lambda_2 = \frac{1}{2}\theta^2\gamma_2 \tag{21}$$

and

$$\lambda_5 = \frac{1}{2}\theta^2\gamma_1 \tag{22}$$

where λ_2 and λ_5 are the last two of four viscosities associated with the nematic-like rotational viscosities of SmC*, γ_1 and γ_2 are the rotational-viscosity coefficients (RVCs) of nematic liquid crystals, and $\theta = \theta(T)$ is the tilt angle, that is, the angle that the director $\hat{n}$ makes with the layer normal.

Recently, a statistical−mechanical approach for the theoretical treatment of rotational viscosity has been proposed.[36,37] As a result, expressions for both γ_1 and γ_2 can be written in the form

$$\gamma_i = \frac{k_B T \rho}{D_\perp} f_i(S_2) \tag{23}$$

where

$$f_i(S_2) = \begin{cases} g(S_2) \rightarrow i = 1 \\ -pS_2 \rightarrow i = 2 \end{cases}$$

Here,

$$g(S_2) = {S_2}^2 \frac{9.54 + 2.77S_2}{2.88 + S_2 + 12.56{S_2}^2 + 4.695{S_2}^3 - 0.74{S_2}^4}$$

$\rho = N/V$ is the particle number density, k_B is the Boltzmann constant, T is the temperature, p is a molecular geometric factor taken as $p = (a^2 - 1)/(a^2 + 1)$, a is the molecular length-to-breadth ratio of the molecule, and $D_\perp$ is the RDC. Thus, according to eqs 21 and 22, λ_i ($i = 2, 5$) are found to be inversely proportional to the RDC, $D_\perp$, which corresponds to molecular tumbling in the SmC* phase. The temperature dependence of the RVCs, λ_i ($i = 2, 5$), is shown in Figure 10a, whereas the values of $\theta(T)$ are shown in Figure 10b. The experimental values of θ (T) were determined by direct ^{2}H NMR measurements in the temperature range corresponding to the SmC* phase of 11EB1M7. [23] The number density ρ of 11EB1M7 (at 339 K ≤ T ≤ 360 K) has been fixed to the value 2×10^{27} m^{-3}, whereas the molecular length-to-breadth ratio was fixed to the value 4.2. Analysis of the calculated data for the RVCs λ_2 and λ_5 shows

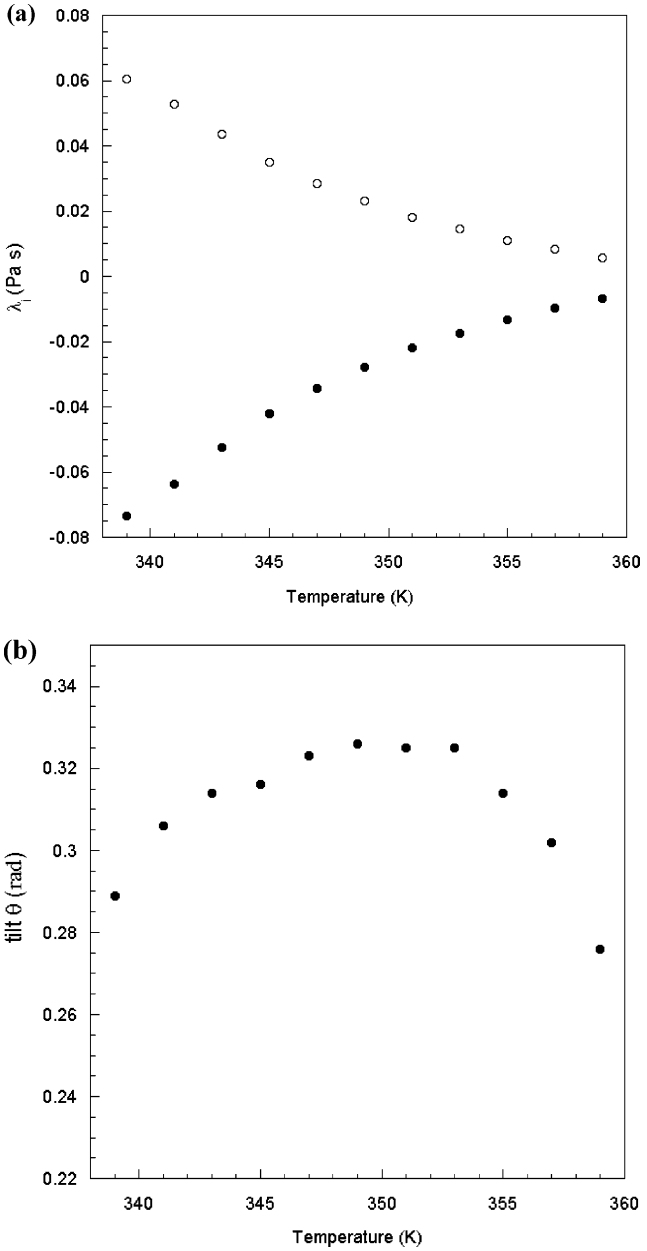

Figure 10. Temperature dependence of λ_2 (full circles) and λ_5 (empty circles) calculated using eqs 19 and 20 (a), at fixed density and values of the $\theta = \theta(T)$, measured by ^{2}H NMR techniques, for 11EB1M7 molecules in the SmC* phase (b).

that $|\lambda_2| > |\lambda_5|$ for the temperature range in which the molecules of 11EB1M7 exhibit the SmC* phase. Physically, this means that in this case the director $\hat{n}$ will align at an angle of $\alpha = {}^1/_2 \cos^{-1}(-\lambda_5/\lambda_2)$ to the shear flow direction.

Conclusions

In this paper, the RDCs for the overall molecular motions ($D_{||}$ and $D_{\perp}$) and internal reorientation around the para axes of the phenyl and biphenyl fragments ($D_{R(biph)}$ and $D_{R(phen)}$) in the SmC* phase of the ferroelectric smectogen 11EB1M7 have been obtained from ^{2}H NMR. The trend of diffusional coefficients has been compared with that found in the SmA phase for the same smectogen, and no significant changes have been observed, except for the tumbling motion, where the activation energy seems to be sensibly higher in the SmC* phase and a significant jump is observed at the phase transition.

In the second part of the paper, the diffusional coefficients, the orientational order S_2, and the tilt angle $\theta(T)$ as determined by ^{2}H NMR techniques have been used to calculate dielectric and viscous properties. In particular, the relaxation times τ^1_{00}, τ^1_{10}, and τ^1_{01} and the longitudinal and transverse components of the real $\mathscr{R}\chi_\gamma(\omega)$ and imaginary $\mathscr{I}\chi_\gamma(\omega)$ ($\gamma = ||, \perp$) parts of the complex susceptibility tensor have been calculated at different temperatures within the SmA phase. We found that the longitudinal component of the loss spectra is characterized by lower frequency peaks compared to the transverse component, and the longitudinal dispersion is characterized by shoulders shifted to the lower frequency region compared to the transverse component of the spectra, which is effectively described by a Debye-type relaxation mechanism. We also show that, under high-shear rates, flow always produces a laminar flow regime, at least for the ferroelectric liquid crystal 11EB1M7 in its SmC* phase.

In this work, a self-consisted dynamic study of the ferroelectric SmC* phase by means of ^{2}H NMR has been presented and discussed. The results obtained in both SmA and SmC* phases by NMR have revealed themselves to be useful in calculating dielectric properties and in validating molecular models in both smectic phases. This is an important step toward the direct comparison between experimental NMR and dielectric relaxation spectroscopies even for ferroelectric mesogens.

Acknowledgment. This work was financially supported by the P.R.I.N. 2003 (Italian MIUR). A.V.Z. gratefully acknowledges the receipt of a senior research fellowship from the Research Council of the K. U. Leuven.

References and Notes

(1) Hoatson, G. L.; Levine, Y. K. A comparative survey of the physical techniques used in studies of molecular dynamics. In *The Molecular Dynamics of Liquid Crystals*; Luckhurst, G. R., Veracini, C. A., Eds.; NATO ASI series; Reidel: Dordrecht, The Netherlands, 1989; Vol. 431, Chapter 1.

(2) Williams, G. Dielectric Relaxation Behaviour of Liquid Crystals. In *The Molecular Dynamics of Liquid Crystals*; Luckhurst, G. R., Veracini, C. A., Eds.; NATO ASI series; Reidel: Dordrecht, The Netherlands, 1989; Vol. 431, Chapter 17.

(3) Urban, S.; Gestblom, B.; Gandolfo, C.; Veracini, C. A. *Z. Naturforsch., A: Phys. Sci.* **2002**, *57*, 819.

(4) Domenici, V.; Czub, J.; Geppi, M.; Gestblom, B.; Urban, S.; Veracini, C. A. *Liq. Cryst.* **2004**, *31*, 91.

(5) Zakharov, A. V.; Ronald, Y.; Dong, R. Y. *Phys. Rev. E: Stat. Nonlinear, Soft Matter Phys.* **2001**, *63*, 011704.

(6) Zakharov, A. V.; Maliniak, A. *Eur. Phys. J. E* **2001**, *4*, 435.

(7) Geppi, M.; Veracini, C. A. Chiral Smectic Phases: NMR studies. In *Encyclopedia of Nuclear Magnetic Resonance*; Grant, M. D., Harris, R. K., Eds.; John Wiley and Sons: Chichester, U.K., 2002; Vol. 9, p 506.

(8) Musevic, I.; Blinc, R.; Zeks, B. *The physic of ferroelectric and antiferroelectric liquid crystals*; World Scientific: Singapore, 2000.

(9) Berggren, E.; Zannoni, C. *J. Chem. Phys.* **1993**, *99*, 6180.

(10) Tarroni, R.; Zannoni, C. *J. Chem. Phys.* **1991**, *95*, 4550.

(11) Domenici, V.; Geppi, M.; Veracini, C. A. *Chem. Phys. Lett.* **2003**, *382*, 518.

(12) Dong, R. Y.; Chen, Y. B.; Veracini, C. A. *Chem. Phys. Lett.* **2005**, *405*, 177.

(13) Domenici, V.; Geppi, M.; Veracini, C. A.; Blinc, R.; Lebar, A.; Zalar, B. *ChemPhysChem* **2004**, *5*, 91.

(14) Vold, R. R. In *Nuclear Magnetic Resonance of Liquid Crystals*; Emsley, J. W., Ed.; Reidel: Dordrecht, The Netherlands, 1985; Chapter 11, pp 253−288.

(15) Berggren, E.; Zannoni, C. *Mol. Phys.* **1995**, *85*, 299.

(16) Beckmann, P. A.; Emsley, J. W.; Luckhurst, G. R.; Turner, D. L. *Mol. Phys.* **1983**, *50*, 699.

(17) Saupe, A. *Z. Naturforsch., A: Phys. Sci.* **1965**, *19*, 161.

(18) Pincus, P. *Solid State Commun.* **1979**, *7*, 415.

(19) Cifelli, M.; Forte, C.; Geppi, M.; Veracini, C. A. *Mol. Cryst. Liq. Cryst.* **2001**, *372*, 81.

(20) Calucci, L.; Geppi, M. *J. Chem. Inf. Comput. Sci.* **2001**, *41*, 1006.

(21) Catalano, D.; Chiezzi, L.; Domenici, V.; Dong, R. Y.; Fodor-Csorba, K.; Geppi, M.; Veracini, C. A. *Macromol. Chem. Phys.* **2002**, *203*, 1594.

(22) Catalano, D.; Cifelli, M.; Fodor-Csorba, K.; Geppi, M.; Gaics-Baitz, E.; Jakli, A.; Veracini, C. A. *Mol. Cryst. Liq. Cryst.* **2000**, *351*, 245.

(23) Catalano, D.; Chiezzi, L.; Domenici, V.; Geppi, M.; Veracini, C. A. *J. Phys. Chem. B* **2003**, *107*, 10104.
(24) Wimperis, S. *J. Magn. Reson.* **1990**, *86*, 46.
(25) Jeener, J.; Broekaert, P. *Phys. Rev.* **1967**, *157*, 232.
(26) Perrin, F. *J. Phys. Radium* **1934**, *5*, 497.
(27) Dozov, I.; Kirov, N.; Fontana, M. P. *J. Chem. Phys.* **1984**, *81*, 2585.
(28) Moro, G.; Nordio, P. L. *Chem. Phys. Lett.* **1983**, *96*, 192.
(29) Thoen, J.; Bose, T. K. In *Handbook of Low and High Dielectric Constant Materials and Their Applications*; Nalwa, H. S., Ed.; Academic Press: New York, 1999; Chapter 11.
(30) Luckhurst, G.; Zannoni, C. *Proc. R. Soc. London, Ser. A* **1975**, *343*, 389.
(31) Leslie, F. M.; Stewart, I. W.; Nakagawa, M. *Mol. Cryst. Liq. Cryst.* **1991**, *198*, 443.
(32) Carlsson, T.; Leslie, F. M.; Clark, N. A. *Phys. Rev. E: Stat. Phys., Plasmas, Fluids, Relat. Interdiscip. Top.* **1995**, *51*, 4509.
(33) Stewart, I. W. *The static and dynamic continuum theory of liquid crystals*; Taylor and Francis: London, 2004.
(34) Ericksen, J. L. *Arch. Ration. Mech. Anal.* **1960**, *4*, 231.
(35) Leslie, F. M. *Arch. Ration. Mech. Anal.* **1968**, *28*, 265.
(36) Kuzuu, N.; Doi, M. *J. Phys. Soc. Jpn.* **1986**, *52*, 3486.
(37) Zakharov, A. V. *Phys. Lett. A* **1994**, *193*, 471.